



## Detecting tropical forest biomass dynamics from repeated airborne lidar measurements

V. Meyer<sup>1</sup>, S. S. Saatchi<sup>1</sup>, J. Chave<sup>2</sup>, J. W. Dalling<sup>3</sup>, S. Bohlman<sup>4</sup>, G. A. Fricker<sup>5</sup>, C. Robinson<sup>5</sup>, M. Neumann<sup>1</sup>, and S. Hubbell<sup>6,7</sup>

<sup>1</sup>Jet Propulsion Laboratory, California Institute of Technology, 4800 Oak Grove Drive, Pasadena, CA 91109, USA

<sup>2</sup>CNRS, Laboratoire Evolution et Diversité Biologique, UMR5174, Université Paul Sabatier, 31062 Toulouse cedex, France

<sup>3</sup>Department of Plant Biology, University of Illinois, Urbana, IL 61801, USA

<sup>4</sup>School of Forest Resources and Conservation, University of Florida, Gainesville, FL 32611, USA

<sup>5</sup>Department of Geography, University of California, Los Angeles, Los Angeles, CA 90095, USA

<sup>6</sup>Department of Ecology and Evolutionary Biology, University of California, Los Angeles, Los Angeles, CA 90095, USA

<sup>7</sup>Center for Tropical Forest Science, Smithsonian Tropical Research Institute, Attn: 9100 Panama City, PL, Washington, DC 20521-9100, USA

Correspondence to: V. Meyer (victoria.meyer@jpl.nasa.gov)

Received: 16 January 2013 – Published in Biogeosciences Discuss.: 5 February 2013

Revised: 20 June 2013 – Accepted: 5 July 2013 – Published: 14 August 2013

**Abstract.** Reducing uncertainty of terrestrial carbon cycle depends strongly on the accurate estimation of changes of global forest carbon stock. However, this is a challenging problem from either ground surveys or remote sensing techniques in tropical forests. Here, we examine the feasibility of estimating changes of tropical forest biomass from two airborne lidar measurements of forest height acquired about 10 yr apart over Barro Colorado Island (BCI), Panama. We used the forest inventory data from the 50 ha Center for Tropical Forest Science (CTFS) plot collected every 5 yr during the study period to calibrate the estimation. We compared two approaches for detecting changes in forest aboveground biomass (AGB): (1) relating changes in lidar height metrics from two sensors directly to changes in ground-estimated biomass; and (2) estimating biomass from each lidar sensor and then computing changes in biomass from the difference of two biomass estimates, using two models, namely one model based on five relative height metrics and the other based only on mean canopy height (MCH). We performed the analysis at different spatial scales from 0.04 ha to 10 ha. Method (1) had large uncertainty in directly detecting biomass changes at scales smaller than 10 ha, but provided detailed information about changes of forest structure. The magnitude of error associated with both the mean biomass stock and mean biomass change de-

clined with increasing spatial scales. Method (2) was accurate at the 1 ha scale to estimate AGB stocks ( $R^2 = 0.7$  and  $RMSE_{\text{mean}} = 27.6 \text{ Mg ha}^{-1}$ ). However, to predict biomass changes, errors became comparable to ground estimates only at a spatial scale of about 10 ha or more. Biomass changes were in the same direction at the spatial scale of 1 ha in 60 to 64 % of the subplots, corresponding to  $p$  values of respectively 0.1 and 0.033. Large errors in estimating biomass changes from lidar data resulted from the uncertainty in detecting changes at 1 ha from ground census data, differences of approximately one year between the ground census and lidar measurements, and differences in sensor characteristics. Our results indicate that the 50 ha BCI plot lost a significant amount of biomass ( $-0.8 \text{ Mg ha}^{-1} \text{ yr}^{-1} \pm 2.2(\text{SD})$ ) over the past decade (2000–2010). Over the entire island and during the same period, mean AGB change was  $0.2 \pm 2.4 \text{ Mg ha}^{-1} \text{ yr}^{-1}$  with old growth forests losing  $-0.7 \text{ Mg ha}^{-1} \text{ yr}^{-1} \pm 2.2(\text{SD})$ , and secondary forests gaining  $+1.8 \text{ Mg ha}^{-1} \text{ yr}^{-1} \pm 3.4(\text{SD})$  biomass. Our analysis suggests that repeated lidar surveys, despite taking measurement with different sensors, can estimate biomass changes in old-growth tropical forests at landscape scales ( $> 10 \text{ ha}$ ).

## 1 Introduction

Tropical forests are a major focus for research not only because of their high biodiversity but also because of the role they play in the global carbon cycle and recently in climate mitigation policies through REDD (Reduced Emissions from Deforestation and Degradation). The study of forest dynamics is of particular interest because changes in carbon fluxes over time are caused by either natural or anthropogenic disturbances and by recovery from these disturbances (Chazdon, 2003). Furthermore, old growth forests may be gaining biomass from potential enhancement of forest productivity due to an increase in atmospheric carbon dioxide or increased nutrient availability (Phillips et al., 1998). Carbon flux measurements in tropical forests have shown major improvements in recent years, based on both ground and remote sensing techniques. For ground-based data, researchers have developed allometric equations from tree inventory data collected from a range of tropical forest types (Chave et al., 2005; Higuchi et al., 1994; Chambers et al., 2001). These equations are key to converting tree diameter, height, and wood-specific gravity into tree aboveground biomass (AGB, measured in oven-dry mass units) and to inferring stand AGB across spatial scales (Chave et al., 2004). However, forest structure and AGB distribution are spatially variable, and inferring large-scale tropical forest carbon dynamics from measurements on a small number of research plots is fraught with difficulties and large uncertainties (Clark and Clark, 2000; Saatchi et al., 2011). Permanent research plots provide accurate estimates of carbon fluxes at the local scale, but their spatial locations may not be representative of forest landscapes, leading to uncertainty in estimates at larger spatial scales.

A number of researchers have shown that remote sensing approaches, particularly from lidar or low-frequency radar sensors, provide relatively accurate estimates of aboveground biomass over large areas (Asner et al., 2010; Drake et al., 2002a; Lefsky et al., 2002; Saatchi et al., 2011). Asner et al. (2011) have demonstrated that high-resolution lidar data from airborne platforms are the most commercially available, cost-effective, and accurate sensor for assessing forest aboveground carbon stock for policy-driven projects. Lidar uses light in the form of a pulsed laser to measure distances to the Earth's surface. Ground elevation and canopy elevation are retrieved from these measurements." Lidar measurements provide three-dimensional forest structure at sufficiently high spatial resolution to capture several important metrics of forest structure and dynamics: (1) tree size structure representing successional stages of the forest (Ni-Meister, et al., 2001), (2) gap size and light conditions in the forest capturing the disturbance dynamics and conditions for forest carbon dynamics (Lefsky et al., 2002; Kellner and Asner, 2009), and (3) spatial patterns representing changes of forest structure and aboveground biomass from tree to landscape scales (Dubayah et al., 2010).

The recent literature on this topic has mostly focused on measuring tropical forest carbon stocks. Comparatively limited research has been devoted to assessing the capability of remote sensing data to detect changes of forest aboveground biomass (see Dubayah et al., 2010). One can use vertical height profiles to develop algorithms for biomass change detection at various spatial scales using small footprint lidar or medium footprint waveform lidar sensors (Dubayah et al., 2010). In this paper, we test this approach over the period 1998–2009 in the tropical forest on Barro Colorado Island (BCI), Panama. We quantify the uncertainty for both AGB stocks and changes at different spatial scales ranging from below 1 ha to 10 ha using two different lidar sensors. The 1998 dataset was acquired by the Land, Vegetation and Ice Sensor (LVIS), which is a medium footprint (20 m) sensor. The 2009 dataset was acquired by a discrete return lidar (DRL), which has a small footprint (25–60 cm). We then quantify the errors related to geolocation, differences between the two sensors, and the errors related to the ground data at different spatial scales and extend the analysis of local scale carbon dynamics in the 50 ha plot to the entire area of Barro Colorado Island. Because LVIS has a footprint that is already the size of the existing 0.04 ha subplots in the 50 ha BCI plot, we would not expect the LVIS results to be accurate for either AGB estimation or in AGB change at or below this spatial scale. From our analysis, we can determine the scale at which we can detect the spatial patterns of forest biomass change while simultaneously providing stable and accurate estimates.

## 2 Materials

### 2.1 Study area and inventory data

Barro Colorado Island (BCI) is a 1500 ha former hilltop, now an island located in artificial Gatun Lake, in the Panama Canal in central Panama. BCI became an island when the Chagres River was dammed in 1910 to complete the Panama Canal (McCullough, 1977). The Smithsonian Tropical Research Institute (STRI) has administered the island for Panama since 1921 as part of the Barro Colorado Nature Monument (BCNM), a protected national biological reserve. Croat (1978) and Leigh (1999) provide detailed descriptions of climate, flora and fauna of BCI. BCI is covered by moist tropical forest with half of the island dominated by old secondary forests (approximately 100 yr old), for the most part in succession from agricultural clearings; the rest of the island is covered by forests relatively undisturbed for the past 200–400 yr except for some minor selective logging (Kenoyer, 1929; Foster, 1982). The forest canopy can attain 35–40 m, although some emergent trees reach 50 m also (Leigh and Wright, 1990; Leigh et al., 2004). The island receives an average of 2600 mm of rainfall per year. A four-month dry season usually begins in January and ends in

April. Preceding this dry season, about 12 % of the canopy species (maximum height > 10 m) lose their leaves (Leigh and Wright, 1990; Condit et al., 2000).

In this study, we used the BCI 50 ha forest dynamics plot managed by the Center for Tropical Forest Science (CTFS) (Condit, 1998; Hubbell et al., 1999, 2005). The plot is located in an area with low elevational variation in the center of the island (Condit, 1995). The inventory data were first collected in 1982 (Hubbell and Foster, 1983), then every five years since 1985, with the most recent census in 2010. We use the census data collected during the 2000, 2005 and 2010 to match the ground measurements with the remote sensing data. Each census included all trees with diameter at breast height (DBH) greater than 1 cm, with measurements made higher on the bole for individuals with buttresses or trunk irregularities. During each census, CTFS staff tag, measure, map and identify all trees and saplings > 1 cm DBH in the 50 ha plot.

## 2.2 Airborne lidar data

Our study uses airborne lidar data acquired by two different sensors flown over BCI approximately 10 yr apart. Both sensors scanned the landscape to measure the surface elevation and the vegetation vertical structure. We used the Laser Vegetation Imaging Sensor (LVIS) medium footprint lidar dataset acquired in March 1998 (20 m footprint) and a small footprint discrete return lidar (DRL) dataset acquired in August and September 2009 (1 m footprint) (Supplementary Material). We produced relative height (RH) quartiles RH25, RH50, RH75 and RH100 for both LVIS and DRL data as well as mean canopy height (MCH) at 0.04, 0.25, and 1 ha resolution over the entire island (Supplementary Material). We created DRL height metrics at 1 ha scale by using the data already aggregated to 20 m to be consistent with LVIS height metrics, calculated from shots having a footprint of 20 m already. The metrics respectively represent the 25 %, 50 %, 75 %, and 100 % percentile of energy from the lidar waveforms developed at each scale of analysis and represent vegetation in the four quartiles of height in the forest. These metrics are useful predictors of aboveground biomass and canopy vertical structure in forest (Drake et al., 2002a, b, 2003; Duong et al., 2008).

We also performed a footprint-by-footprint analysis to compare the relative height metrics of the two sensors. We extracted DRL relative height metrics at the footprint level from 20 m diameter circular areas in the 1 m DRL data for each LVIS shot location. We used a nearest neighbor analysis to develop correspondence between the center location of LVIS shots and the DRL pixel before extracting the DRL data. We expect approximately 2 m relative error in locating the LVIS shots within the DRL data due to LVIS geolocation and range inaccuracies (Hofton et al., 2002).

Several differences in DRL and LVIS measurements may affect the relative ability of the two different sensors to de-

tect changes. Although LVIS is an imaging lidar, the images are made of discrete footprints scanned across the lidar track. The LVIS footprint is about 20–25 m depending on the altitude of the aircraft. DRL is a small-footprint ( $\sim 50$  cm) imaging lidar with a smaller track and a larger field of view. In both datasets, flight path irregularities, density of LVIS shots and DRL point clouds from overlap, cloud cover, point errors and noise in the data introduce uncertainties in quantifying the canopy and ground elevation: (1) LVIS detection of canopy height is different from DRL largely due to sensor characteristics (Supplement Table S1). In LVIS medium-size footprint, the canopy return is found by starting at the leading edge of the return until a signal greater than some noise threshold is found (Dubayah et al., 2010). The leading edge is the highest reflecting surface height associated with enough canopy material (about  $0.5 \text{ m}^2$ ). In DRL data, the first point return is associated with the highest height of the point cloud data within a nominal grid cell ( $1 \text{ m}^2$ ). The top canopy height from LVIS should be slightly lower than DRL ( $\sim 0.5$  m). This difference is not cross-calibrated in the datasets and may impact the detection of changes due to biomass changes. (2) LVIS detection of the ground elevation is different from DRL. Ground return in LVIS is usually strong, but there are always some shots with errors in detecting the ground elevation due to weak returns from dense canopy. This can cause difficulties in detecting the ground elevation using an automatic processing algorithm, as well as slope effect within the LVIS footprint. DRL is higher in resolution and provides more accurate measurements of ground elevation. However, classifying DRL point clouds for the ground elevation can be erroneous due to small number of point clouds, return of lidar photons from mid-canopy due to vegetation density, and other errors due to pointing, geolocation, and interpolation of last returns. Figure 1 shows a comparison of the ground and canopy elevation (RH100<sub>E</sub>) between the two sensors. We used 3077 shots of LVIS within the 50 ha plot and extracted the corresponding DRL shots over the LVIS shots using a nearest neighbor approach. We used the footprint level data from LVIS and DRL to perform the AGB change detection and used aggregated values of footprints at 1 ha to develop the AGB estimation from LVIS.

We performed a cross-calibration between the two datasets using a filter to improve the LVIS ground elevation estimation using the DRL digital elevation model (DEM) (Fricker et al., 2012) (Supplement, Fig. S1). After calibration, LVIS's height metrics were adjusted to allow comparisons between the two datasets and to detect changes of forest structure and biomass over the landscape and at different spatial scales. The DRL data did not need any further calibration. All LVIS height metrics were adjusted for the errors in ground elevation to allow a comparative analysis of AGB estimation for each dataset. The height metrics are correlated despite capturing different vertical structural characteristics of the forest (Fig. S2).

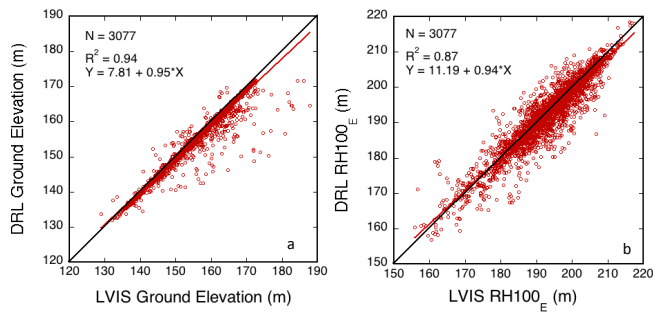


**Fig. 1.** Relationship between LVIS ground elevation and DRL ground elevation, and between LVIS top canopy elevation and DRL top canopy elevation.

### 3 Methods

#### 3.1 Field estimation of AGB change

We used the AGB estimates for a three-census period including the most recent one in 2010 to quantify biomass change within the 50 ha plot at the three spatial scales mentioned above. We used the allometric equation developed by Chave et al. (2005) from a pan-tropical moist forest dataset to make the AGB estimates. The AGB estimate is derived from tree DBH, height and wood-specific gravity. Height was inferred from DBH using species-specific equations (Fig. S3). Here, we only included the trees with DBH > 10 cm for AGB estimation, which represent about 10 % of all trees in the plot.

To compute forest aboveground biomass stock and change, we divided the 50 ha plot into subplots at three spatial scales: 0.04 ha (20 m × 20 m), 0.25 ha (50 m × 50 m) and 1 ha (100 m × 100 m). Each subplot was identified by the coordinates of its four corners and was co-located on the remote sensing data for further analysis.

We calculated AGB estimates from DBH measurements, height estimates (Bohman et al., 2006), and the allometric model (Table S2). We then used ground-estimated AGB to determine AGB change in the 50 ha plot between 2000 and 2010, using the plot census data from 2000, 2005 and 2010. We repeated this analysis at three spatial scales using the mean AGB density and other statistics to quantify the changes of biomass density through time and the uncertainty associated with estimating changes from census data. We propagated errors associated with estimating AGB from tree allometry to the plot size and used the errors to estimate the uncertainty of ground estimation of biomass change.

#### 3.2 Lidar estimation of AGB change

We developed two types of analyses using the 1998 and 2009 lidar datasets: (1) we used the difference between the height metrics from the two sensors and related those to changes of AGB at 1 ha. We refer to this method as the direct estimation of AGB change. (2) We estimated biomass from LVIS and

DRL height metrics separately for each period and examined the difference between the two estimates to quantify biomass change. We refer to this method as the indirect estimation of AGB change. Both approaches focused on the 1 ha scale to perform the change analysis because of the larger uncertainties associated with smaller plot size and LVIS sampling data.

##### 3.2.1 Direct estimation of biomass change

Because intermediate height metrics (RH25, RH50 and RH75) from LVIS and DRL are different (Supplementary Material) and there are potential errors introduced by ground-finding algorithms in both sensors, we developed a footprint-level analysis with canopy elevation metrics such as RH100<sub>E</sub> and MCH<sub>E</sub>, where RH100<sub>E</sub> is the elevation of the maximum canopy height and MCH<sub>E</sub> corresponds to the elevation of the mean canopy height. These metrics are not defined relative to the ground and are therefore not affected by errors in ground-finding. We tested differences in these height metrics between the two surveys ( $\Delta$ RH100<sub>E</sub> and  $\Delta$ MCH<sub>E</sub>) against differences in biomass between 2000 and 2010 ( $\Delta$ AGB<sub>gnd</sub>).

The direct method allows us to use the most fundamental lidar measurements (RH100<sub>E</sub>) in estimating AGB change. Other height metrics are energy-based and depend on sensor characteristics.

We used a linear relationship between the  $\Delta$ AGB<sub>gnd</sub> and  $\Delta$ RH100<sub>E</sub> and  $\Delta$ MCH<sub>E</sub> at the 1 ha scale to examine the prediction of AGB change directly from changes in lidar metrics and to quantify the efficacy of the approach for mapping larger areas (> 1 ha).

##### 3.2.2 Indirect estimation of biomass change

We used the field-estimated AGB for the 2000 and 2010 censuses in a model using lidar metrics from the 1998 LVIS and 2009 DRL to estimate AGB from lidar for each period. In developing estimation models for lidar data, we did not attempt to adjust the ground biomass data to match the year of lidar flights because doing so would introduce errors due to uncertainty in forest growth and disturbance rates.

We developed models between lidar metrics and AGB at each scale using a power law function. We used a relative importance analysis to evaluate the importance of each variable in explaining the variability of biomass at different scales. We also performed a model selection using the Akaike information criterion (AIC). The analysis was performed in the R statistical computing environment. A relative importance analysis quantifies the portion of the coefficient of determination ( $R^2$ ) attributable to the parameter (as predictor) when the parameters are correlated in the regression analysis (Chao et al., 2008). Testing for the relative importance of each height metric, we found that all five metrics (RH25, RH50, RH75, MCH and RH100) together explained about 75 % of the variation in forest biomass at 1 ha scale for both LVIS and DRL,

**Table 1.** Relative importance of each metric in a power law model (1 ha scale). All five metrics together explain 75 % of the model. MCH has the highest relative importance for both LVIS and DRL models.

Metrics	Relative importance in % (LVIS)	Relative importance in % (DRL)
RH25	11	14
RH50	14	17
RH75	16	16
MCH	18	17
RH100	16	12

and relatively less variation at 0.25 ha (50–58 %) and 0.04 ha (20–29 %). Table 1 presents the relative contribution of the height metrics at 1 ha. We found that MCH was the metric with the highest relative contribution for both LVIS and DRL (with RH50 for DRL). The AIC analysis showed that MCH is also a better fit than the other relative height metrics when using a single metric in our model (Table 2), confirming results from previous studies (Mascaro et al., 2011a) as well as studies in other tropical forests (Dubayah et al., 2010; Asner et al., 2011). AIC showed that models using less than five metrics may provide better fits than using all five metrics (Table 2). However, note that overall, all the models tested have similar AIC scores. We developed two models based on these results. The first model uses all five available metrics because one of the main goals of this study is to have a common measurement framework for both sensors. Using fewer metrics in our model would mean that different metrics should be selected for LVIS and DRL, based on the relative importance and AIC analyses. Therefore, we used a model with all five relative metrics and a power law function between the metrics and biomass (thereafter called 5RH model) to estimate AGB from lidar data at three spatial scales of 0.04 ha, 0.25 ha, and 1 ha. (Fig. S4).

$$AGB_{est} = a_0 + a_1RH25^\alpha + a_2RH50^\beta + a_3RH75^\gamma + a_4MCH^\delta + a_5RH100^\epsilon \quad (1)$$

where the coefficients are inferred from the fitting model using LVIS and DRL data separately (Table S3).  $RMSE_{LVIS}$  is  $28.1 \text{ Mg ha}^{-1}$  and  $RMSE_{DRL}$  is  $27.1 \text{ Mg ha}^{-1}$  at 1 ha.

The second model uses MCH as the main variable (thereafter called MCH model), in which the coefficients were found to be almost exactly the same for LVIS and DRL (Fig. 2):

$$AGB_{est} = a \times MCH^b, \quad (2)$$

where  $a = 0.11$  for LVIS and  $a = 0.12$  for DRL, and  $b = 2.14$  for both.

$RMSE_{LVIS}$  is  $28.2 \text{ Mg ha}^{-1}$  and  $RMSE_{DRL}$  is  $28.9 \text{ Mg ha}^{-1}$  at 1 ha.

We present and discuss the results from both models.

**Table 2.** Akaike information criterion (AIC). The smaller the AIC, the better the fit.

Metrics used in model	AIC (LVIS)	AIC (DRL)
RH25, RH50, RH75, MCH, RH100	480	476.4
RH50, RH75, MCH, RH100	478.2	474.5
RH25, RH50, RH75, MCH	484.8	475.4
RH50, RH75, MCH	483.3	473.6
RH50, MCH	481.5	475.5
RH75, MCH	481.5	478.4
RH50, RH75	486.5	481.2
RH25	507.3	486.8
RH50	496.5	479.3
MCH	479.5	478.5
RH75	486.2	480.9
RH100	500.8	502.5

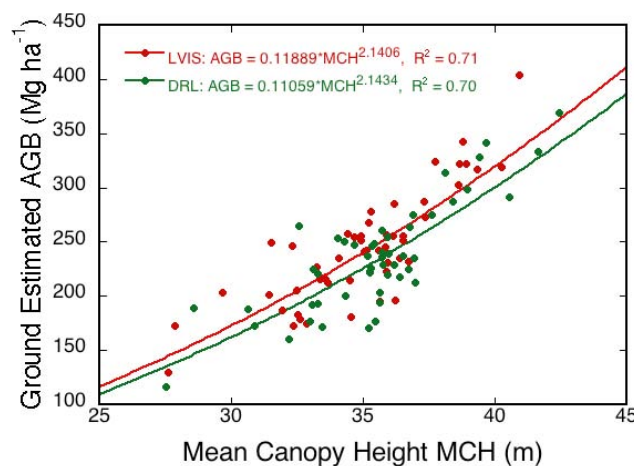


**Fig. 2.** Relationship between ground-estimated AGB and MCH from LVIS and DRL, at 1 ha. The coefficients of the two equations are very similar.

A “leave-20 %-out” cross-validation was performed to assess the predictive performance of our models with both lidar sensors. This cross-validation uses 20 % of the original data as the validation data, while the remaining 80 % are used as the training data. This operation is repeated until all the observations are used as the validation data once. This method is similar to the  $K$ -fold cross-validation method, where  $K = 5$ . The 1 ha scale AGB results were then aggregated to get values at larger scales (5 ha, 10 ha and 25 ha). Due to the low number of values at larger scales for performing the statistical analysis, we only report the comparison of aggregated numbers with the field observations.

We then extended the analysis by calculating the AGB change over the entire island from the two maps generated from each lidar sensor. The results section reports on maps derived from both approaches at 1 ha scale over the 50 ha CTFS plot using Eqs. (1) and (2). We compare the spatial distribution of AGB change derived from lidar data with ground

**Table 3.** 2010 AGB statistics, from field estimations. AGB is highly variable and its distribution is skewed toward low values when using 0.04 ha subplots, but becomes more stable at 0.25 ha and 1 ha.

AGB 2010 (Mg ha <sup>-1</sup> )	0.04 ha	0.25 ha	1 ha
Mean	235.65	235.65	235.65
Standard deviation	204.77	83.04	49.61
Skewness	3.05	0.78	0.45
Kurtosis	13.65	0.46	0.52
Min	21.6	88.60	116.14
Max	1838.92	567.21	369.13
Coefficient of variation	0.87	0.35	0.21

estimation and evaluate the uncertainty in predicting AGB change. To relate the changes of the forest AGB to landscape features, we further analyzed the change map by classifying the forests of the island into two age groups, based on an available forest age map (Mascaro et al., 2011a, from Enders, 1935). The age groups included areas of forest older than 400 yr, hereafter called “old growth forest”, and areas of forest younger than 130 yr, classified as “secondary forest”. Using the age map, we analyzed the magnitude and spatial patterns of the forest biomass change over the island.

## 4 Results

### 4.1 Field estimates of forest biomass dynamics

The analysis of the spatial structure of the forest within the 50 ha permanent plot shows that 1 ha subplots give stable estimates of AGB with low spatial variance, while at 0.04 ha subplots estimates of AGB have high spatial variability dominated by the spatial variability of large trees. In 2010, AGB ranged between 21 and 1838 Mg ha<sup>-1</sup> in 0.04 ha subplots (coefficient of variation = 0.75), showing high AGB variation, compared to 116 to 369 Mg ha<sup>-1</sup> in 1 ha subplots (coefficient of variation = 0.18) (Table 3). The AGB distribution (Fig. S5) is skewed towards low biomass values in the case of small subplots of 0.04 ha (skewness = 3.05) but is more symmetrical in the case of 1 ha subplots (skewness = 0.45). The presence or absence of a single large tree in a 0.04 ha subplot strongly impacts the AGB value of a subplot, leading to very low or very high AGB values (Chave et al., 2003).

AGB, estimated at the 1 ha scale, decreased both from 2000 to 2005 and from 2005 to 2010 census periods in the 50 ha plot (Fig. S5b, Table 4). Changes from 2000 and 2005 were slightly skewed to negative values and had only few extreme values (mean =  $-2.4 \text{ Mg ha}^{-1} \pm 10.5 \text{ (SD)}$ ), whereas during the second period between 2005 and 2010, there were more extreme values and the biomass loss was larger (mean =  $-5.5 \text{ Mg ha}^{-1} \pm 16.1 \text{ (SD)}$ ). AGB in the 50 ha plot dropped by  $7.8 \text{ Mg ha}^{-1} \pm 17.6 \text{ SD}$  over the 10 yr period of study (i.e., an average decline of  $-0.8 \text{ Mg ha}^{-1} \text{ yr}^{-1}$ ).

The spatial scale analysis of AGB change (Table 4) confirms that, at the 1 ha scale, the observed changes are more stable for a long-term analysis than smaller subplots ( $\text{SD}_{\text{change2000/2010.1ha}} = 17.6 \text{ Mg ha}^{-1}$  and  $\text{SD}_{\text{change2000/2010.0.04ha}} = 107.4 \text{ Mg ha}^{-1}$ ). Here, stability refers to less variability and suggests that larger plots are individually more reliable for detecting long-term changes, whereas smaller plots individually represent changes associated with both natural gap dynamics (disturbance and recovery) and long-term changes. Furthermore, 37 1 ha subplots lost AGB and the rest gained AGB over the same period (Fig. 3). By further aggregating the subplots to larger scales, we find the forest is losing biomass more uniformly at 5 ha scale ( $\text{SD} = 5.9 \text{ Mg ha}^{-1}$ ), and at 10 ha scale ( $\text{SD} = 4.2 \text{ Mg ha}^{-1}$ ). At 25 ha, the two subplots lost 7.7 and 8.0 Mg ha<sup>-1</sup> of AGB for an average value of 7.8 Mg ha<sup>-1</sup> at 50 ha between 2000 and 2010.

### 4.2 Lidar estimation of height change

The direct measurement of change starts with the observation of canopy structure from both sensors. We used the canopy maximum height above the ellipsoid to detect changes between the two dates and sensors. The RH100<sub>E</sub> from LVIS and DRL may be compared at the footprint level and used to detect changes in terms of canopy height. Figure 4 shows that canopy height globally decreased in the 50 ha plot from 1998 (LVIS) to 2009 (DRL). Mean difference between RH100<sub>E</sub> DRL and RH100<sub>E</sub> LVIS within the 50 ha plot is  $-1.1 \text{ m} \pm 3.4 \text{ (SD)}$ , with 60 % of the 3077 LVIS shots landing in the plot showing lower canopy height in 2009 than in 1998. The footprint-by-footprint analysis shows that 8 % (260 shots) had a drop of more than 5 m in RH100<sub>E</sub> between 1998 and 2009, while 4 % (123 shots) had increased by more than 5 m RH100<sub>E</sub> in 2009 (Fig. 4a). Figure 4b shows that the distribution of RH100<sub>E</sub> DRL is slightly shifted towards lower values than RH100<sub>E</sub> LVIS (mean RH100<sub>E</sub> LVIS =  $192.7 \text{ m} \pm 9.4 \text{ (SD)}$ , mean RH100<sub>E</sub> DRL =  $191.6 \text{ m} \pm 9.4 \text{ (SD)}$ ).

### 4.3 Lidar-derived biomass estimates

The influence of spatial scale on AGB is examined here by again comparing the results obtained using 0.04 ha, 0.025 ha and 1 ha subplots, using the cross-validated data. Results are presented for our two approaches: (1) using the five available RH metrics and (2) using MCH only. Figure 5 (5RH approach) and Figure S6 (MCH approach) show that, for both LVIS and DRL data, the accuracy of AGB estimation increases when larger subplots are used. We found similar results for both LVIS and DRL data regarding the relationship between ground AGB and lidar-estimated AGB when using 1 ha subplots in the model. Using all five metrics in the regression model gives a  $R^2$  of 0.70 for both LVIS and DRL ( $R^2 = 0.75$  when using the whole dataset), with a  $p$  value  $< 0.0001$ . The MCH model gives  $R^2_{\text{LVIS}} = 0.70$

**Table 4.** AGB change (in Mg ha<sup>-1</sup>) between 2000, 2005 and 2010, from field estimations, at three spatial scales. AGB decreased both between 2000 and 2005 and between 2005 and 2010 census periods in the 50 ha plot. AGB changes are more stable at 1 ha than at 0.04 ha.

	0.04 ha			0.25 ha			1 ha		
Time period	2000/2005	2005/2010	2000/2010	2000/2005	2005/2010	2000/2010	2000/2005	2005/2010	2000/2010
Mean change	-2.4	-5.5	-7.8	-2.4	-5.5	-7.8	-2.4	-5.5	-7.8
Std Dev.	58.6	93.6	107.4	24.7	37.7	41.7	10.6	16.1	17.6
Min change	-701.7	-1749.3	-1522.7	-145.8	-288.9	-252.0	-44.4	-49.6	-47.0
Max change	237.9	1167.9	1196.4	37.0	177.9	172.1	11.2	45.7	40.3

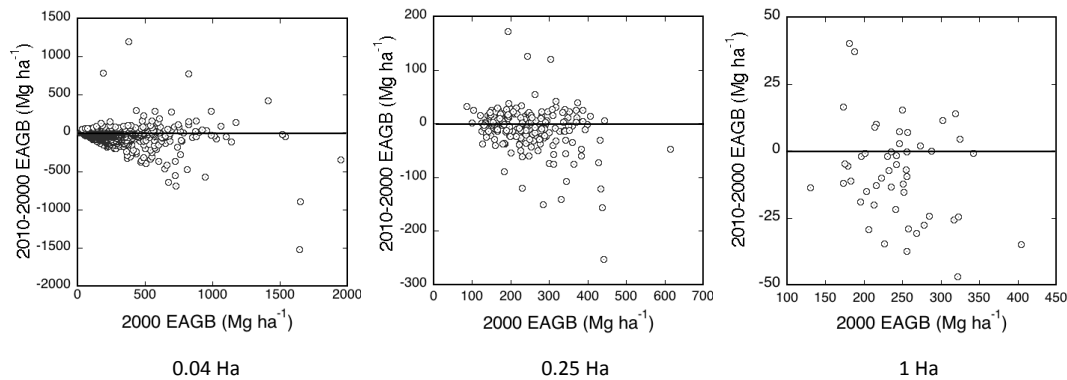


**Fig. 3.** Ground AGB change between 2000 and 2010 at 0.04 ha (left), 0.25 ha (center) and 1 ha (right). Subplots having high AGB in 2000 are losing biomass.

and  $R^2_{DRL} = 0.66$ , with  $p$  value  $< 0.0001$ . When using the whole dataset,  $R^2_{LVIS} = 0.71$  and  $R^2_{DRL} = 0.70$  in the MCH model. For both approaches, RMSE varies between 27.1 and 28.9 Mg ha<sup>-1</sup>. Bias is lower when using all the metrics in our model ( $B_{5RH} < -0.45$  Mg ha<sup>-1</sup>,  $B_{MCH} > 2.13$  Mg ha<sup>-1</sup>).

At the 0.04 ha scale, the estimation accuracy is lower than at the 1 ha scale ( $R^2_{LVIS} = 0.19$  and  $0.18$  and  $R^2_{DRL} = 0.28$ ). At this scale, RMSE is large, varying between 173.8 and 195.4 Mg ha<sup>-1</sup>. Bias stays low in the 5RH approach, but it reaches between 48.7 Mg ha<sup>-1</sup> (for LVIS) and 40.5 Mg ha<sup>-1</sup> (for DRL) when using the MCH approach at 0.04 ha subplots ( $p$  value  $< 0.0001$ ). Although DRL has a higher resolution, DRL-derived AGB estimation at small scales is not more accurate than LVIS. It shows that lidar should not be used to estimate AGB at these resolutions.

#### 4.4 Lidar-derived biomass change

Since lidar does not estimate AGB accurately at spatial scales below 1 ha, only the results at the 1 ha scale are presented here.

##### 4.4.1 Direct estimation of AGB change

Although one would expect biomass change to correlate with change in height metrics, differences in one height metric derived from lidar waveforms ( $\Delta RH_{100E}$  and  $\Delta MCH_E$ ) had no significant relationship ( $R^2 < 0.1$ ) with differences

in forest biomass derived from the analysis of field surveys ( $\Delta AGB_{\text{grd}}$ ). This result suggests that we cannot map the changes of forest biomass by directly analyzing the lidar heights at 1 ha scale using two different sensors. However, using the same sensor for both dates may provide a more reliable measure of height difference with which to calculate AGB change directly from lidar (Dubayah et al., 2010).

##### 4.4.2 Indirect estimation of AGB change

Over the 50 ha plot, both ground and lidar analyses indicate that, on average, AGB decreased by 7.8 Mg ha<sup>-1</sup> between 2000 and 2010. This close match is unsurprising because lidar biomass estimations are calibrated using the ground data. It is therefore expected to have the same average change over the whole 50 ha plot. At the 1 ha scale, the noise caused by estimation errors due to our regression model was large and only biomass changes greater than 18.5 Mg ha<sup>-1</sup> (5RH approach) or 15.8 Mg ha<sup>-1</sup> (MCH approach) could be detected unambiguously from lidar data (standard deviation of lidar-derived AGB change).

Here, we first present the results using the 5RH approach. A total of 30 of the 50 subplots show the same direction of change (7 subplots showing biomass gain and 23 subplots showing biomass loss between the 2 dates) when comparing the ground- and lidar-estimated AGB change (Fig. 6), ignoring the 18.5 Mg ha<sup>-1</sup> threshold ( $p$  value = 0.1). In 15 of the plots that do not show the same direction of change,

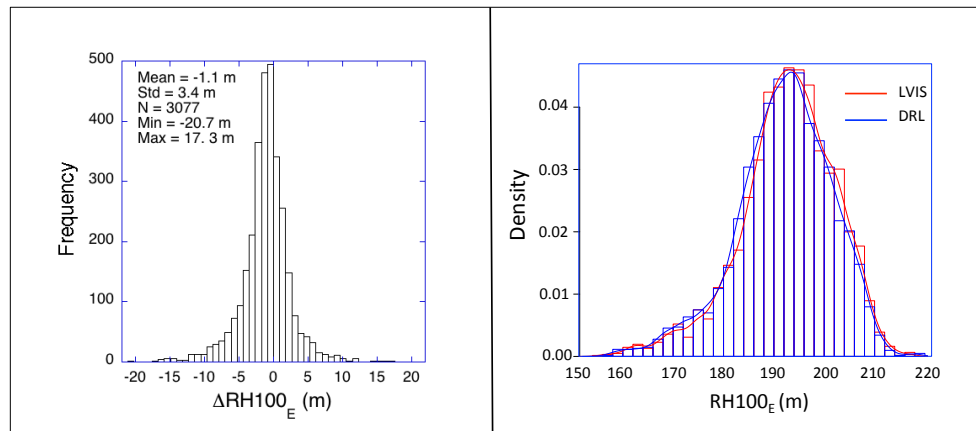


**Fig. 4.** Distribution of RH100E change between 1998 (LVIS) and 2009 (DRL) (left), and distribution of RH100E for each date (right). Both histograms show that top canopy elevation decreased between the two surveys.

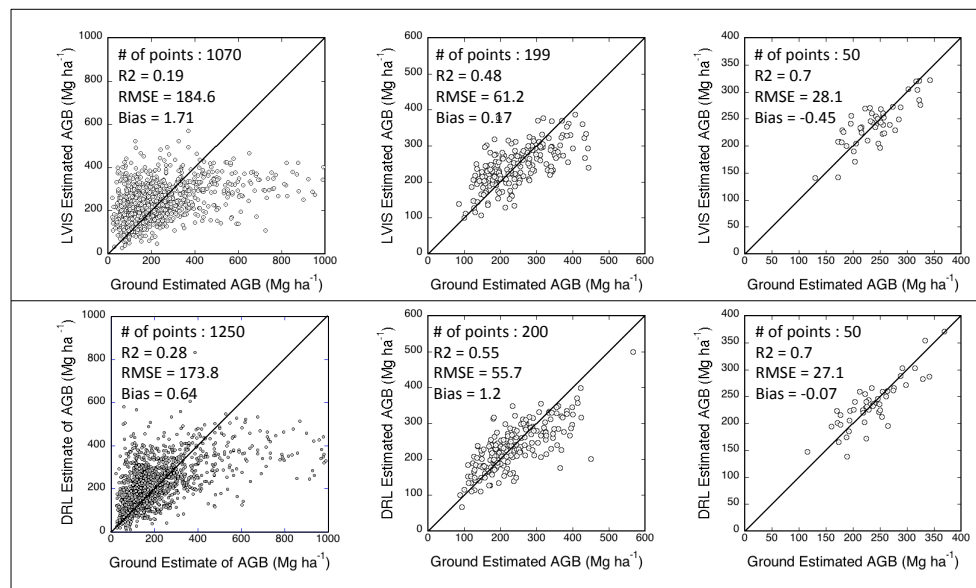


**Fig. 5.** Relationship between ground-estimated AGB and lidar-estimated AGB (top : LVIS, bottom : DRL), using five height metrics in the regression model. The correlation between the two estimations of AGB increases as the scale becomes coarser.

absolute AGB change values are smaller than 18.5 ha in both ground and lidar estimations, and therefore are not considered to have significantly changed. The remaining five plots that do not show the same direction of change have significant change in either or both ground and lidar estimations. Results are similar when only using MCH to estimate AGB. A total of 32 of the 50 subplots showed the same direction (biomass gain or loss between the two dates) comparing the ground- and lidar-estimated AGB change (Fig. 6), ignoring the 15.8 Mg ha<sup>-1</sup> threshold ( $p$  value = 0.03). For 9 of the remaining 18 plots, AGB change between 2000 and 2010 was smaller than 15.8 Mg ha<sup>-1</sup> and therefore within the uncertainty threshold, in both ground and lidar estimations. The remaining 9 subplots showed significantly opposite directions

in lidar and ground estimations. Figure 7 shows where these 1 ha subplots are located within the 50 ha plot.

The ground and lidar detection of changes showed a tighter match when the subplot size increased. At a 10 ha scale, the estimation of change could be predicted to within 6 Mg ha<sup>-1</sup> over 10 yr, or less than 1 Mg ha<sup>-1</sup> yr<sup>-1</sup>. Table 5 shows how spatial scale affects lidar-derived AGB estimations at the plot level. Results are shown with regard to the 5RH approach, but the MCH approach results are similar at these spatial scales. Both lidar-derived AGB change and the difference between lidar and field estimates decreased as the scale became coarser. The range of variance between field-estimated change and lidar-estimated change decreased quickly with increasing scale of analysis, going

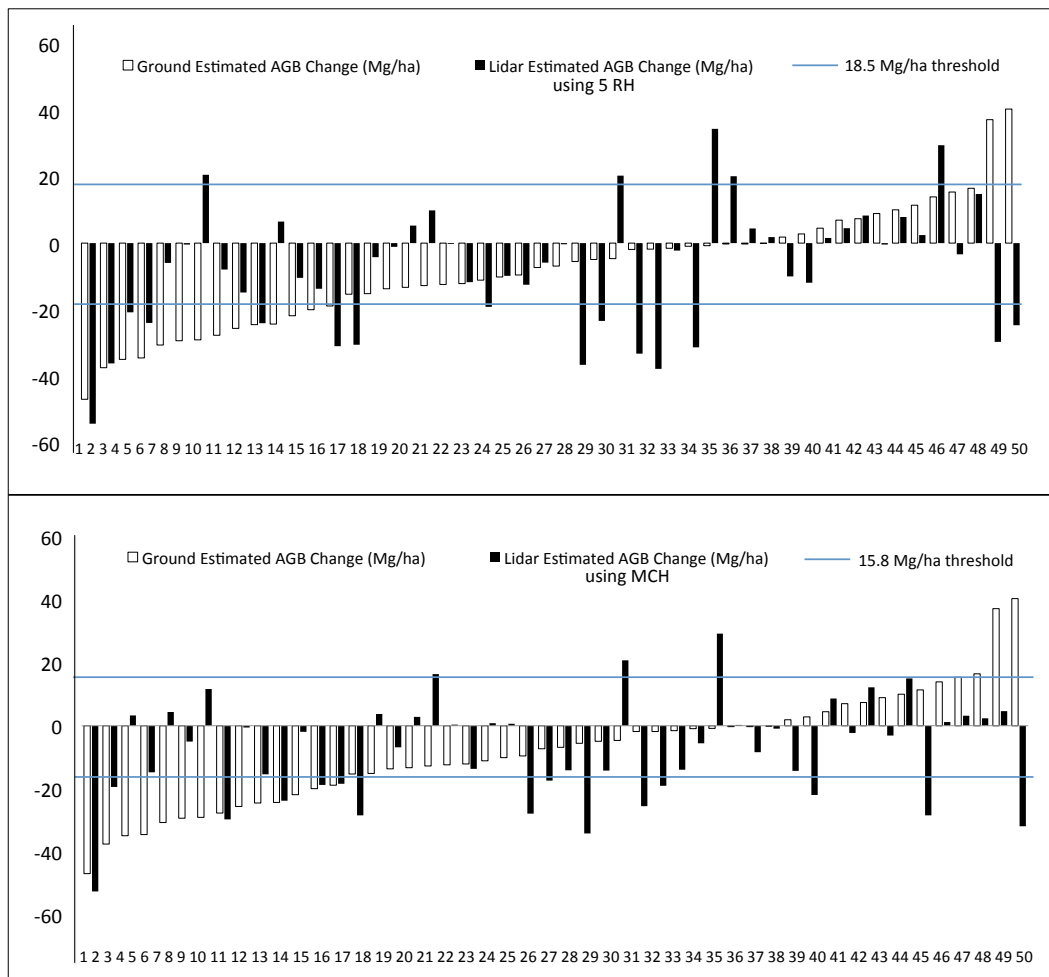


**Fig. 6.** Comparison of AGB change (ground estimation vs. lidar estimation) for every 1 ha subplot using the 5RH approach (top) and the MCH approach (bottom). The sign of AGB change was correctly predicted for 30 and 32 of the 50 subplots.

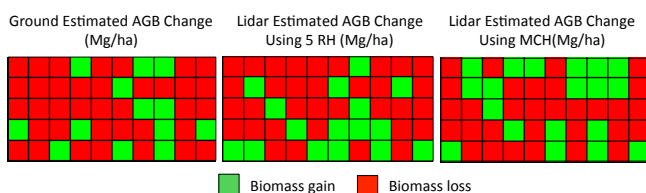


**Fig. 7.** AGB change (in  $\text{Mg ha}^{-1}$ ) from ground estimations (a) and from lidar estimations (b and c) in the 50 ha plot at 1 ha spatial scale. lidar estimates do not clearly show the same AGB change trends as the ground estimates.

from  $\pm 6.7 \text{ Mg ha}^{-1}$  at 1 ha to  $\pm 0.1 \text{ Mg ha}^{-1}$  at 25 ha. These results show that large spatial scales such as 10 ha or 25 ha give accurate AGB change estimations when looking at the 50 ha plot, but the 1 ha scale still seems to be a good option when looking for spatial patterns.

#### 4.4.3 Landscape variation in AGB change

Estimated AGB stocks and changes were mapped across the entire island (1500 ha) using the equations developed at the plot level at 1 ha resolution, for both LVIS and DRL data. These two maps were then used to create an AGB change map (Fig. 8). A mask consisting of a one pixel erosion was applied to the final map to avoid errors induced by edge effects. Hence, all the pixels that were on the edges of the island and contained errors were removed. First, we present the results obtained using all five metrics in our model (Fig. 8a). Mean AGB change over the whole island was found to be  $1.5 \text{ Mg ha}^{-1} \pm 20.4$  (SD), or  $0.2 \text{ Mg ha}^{-1} \text{ yr}^{-1}$ . The map shows that 35 % of the island significantly gained biomass, while 26 % lost biomass. The remaining 39 % did not show any significant change. Patterns related to forest age (Fig. 8c) and stage of regeneration can be seen in the AGB change map. Old growth forest lost biomass ( $\Delta \text{AGB}_{\text{Old}} = -6.8 \text{ Mg ha}^{-1} \pm 22.3$  (SD)), while secondary

**Table 5.** lidar-detected AGB change (in  $\text{Mg ha}^{-1} \text{yr}^{-1}$ ) and the difference between lidar and field AGB change estimates in the 50 ha plot, at large plot scales. Both AGB change and the difference between lidar and field estimates decrease as the scale becomes coarser.

	lidar-detected AGB change (mean = $-0.77$ )		Difference between lidar-detected AGB change and field estimations (mean = $0.02$ )	
	Min	Max	Min	Max
1 ha	-5.26	42.92	-4.97	7.22
5 ha	-2.04	-0.16	-0.75	1.07
10 ha	-1.3	-0.26	-0.69	0.75
25 ha	-0.77	-0.26	-0.5	0.5

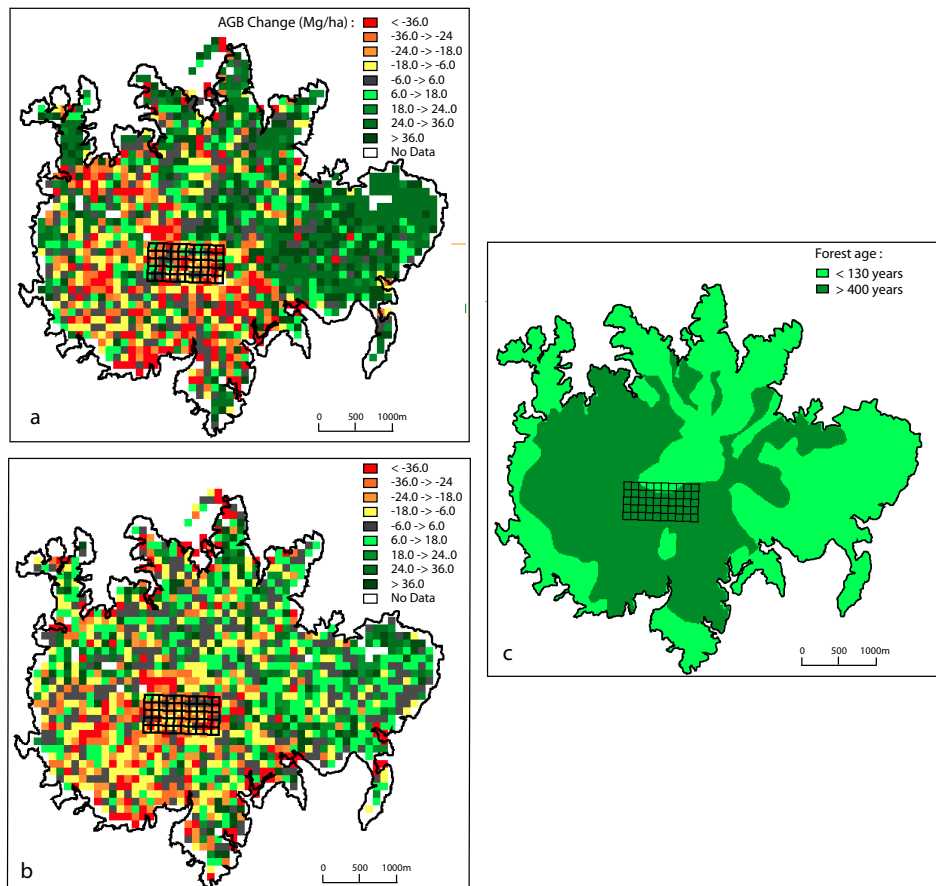


**Fig. 8.** AGB change maps between 2000 and 2010 (a and b) and forest age map (c). The AGB change map from the 5RH approach (a) shows patterns of forest age more clearly than the AGB change map from the MCH approach (b). Globally, AGB decreased in old growth forest (dark green in the age map), whereas the forest gained biomass in younger, regenerating forest (light green in the age map).

forest gained biomass ( $\Delta\text{AGB}_{\text{Sec}} = 18.4 \text{ Mg ha}^{-1} \pm 33.6$  (SD)). The results show that 73 % of the 1 ha areas that lost more than  $18.5 \text{ Mg ha}^{-1}$  (standard deviation of lidar-derived AGB change for this model) are located in old growth forest, while the remaining 27 % are located in secondary forest. Inversely, only 26 % of the 1 ha areas that gained more than  $18.5 \text{ Mg ha}^{-1}$  are located in old growth forest, while the remaining 74 % are located in secondary forest.

We found that using MCH as a single metric in our model tends to give lower values of AGB change (both loss and gain), especially in secondary forest (Fig. 8b). Mean AGB change over the whole island was found to be  $-3.1 \text{ Mg ha}^{-1} \pm 23.8$  (SD), or  $-0.3 \text{ Mg ha}^{-1} \text{yr}^{-1}$ . The AGB change map obtained with the MCH model shows that 15 % of the island had gained biomass between 2000 and 2010, while 25 % lost biomass. The remaining

60 % did not show significant trends during the period (changes less than  $\pm 15.8 \text{ Mg ha}^{-1}$ ). Old growth forest areas lost AGB ( $\Delta \text{AGB}_{\text{Old}} = -4.7 \text{ Mg ha}^{-1} \pm 22.3 \text{ (SD)}$ ), whereas secondary forests stayed neutral ( $\Delta \text{AGB}_{\text{Sec}} = 0.4 \text{ Mg ha}^{-1} \pm 22.5 \text{ (SD)}$ ) between 2000 and 2010. The results show that 63 % of the 1 ha areas that lost more than  $15.8 \text{ Mg ha}^{-1}$  are located in old growth forest, while the remaining 37 % are located in secondary forest. Inversely, 36 % of the 1 ha areas that gained more than  $15.8 \text{ Mg ha}^{-1}$  are located in old growth forest, while the remaining 64 % are located in secondary forest.

## 5 Discussion

The goal of this contribution was to study the ability of lidar technology to estimate and map AGB changes when calibrated and combined with the field data. The relationship between lidar-derived vertical canopy distribution and ground-based estimated AGB at the plot level was used to create predictive equations for AGB at the landscape scale. A large number of studies have recently focused on AGB estimations in tropical forest using lidar technology (Drake et al., 2002a; Asner et al., 2011; Mascaro et al., 2011b; Vincent et al., 2012), but to our knowledge only one has been able to detect AGB changes from repeated lidar measurements (Dubayah et al., 2010). Moreover, Dubayah et al. (2010) used the same sensor to detect AGB changes, whereas this study is the first to use two different sensors, which represents a more realistic case in many applications. Here we review our findings and discuss them in light of this recent literature and address the following question: with what accuracy and at what spatial scale can changes of tropical forest biomass be detected by repeated measurements of lidar profiles?

We quantified a loss of approximately  $0.8 \text{ Mg ha}^{-1} \text{ yr}^{-1}$  of forest aboveground biomass over the 50 ha CTFS plot on BCI over a period of 10 yr. This loss of biomass, although from only one site, can imply significant carbon loss over a large region if extended. Our estimate of carbon loss contrasts with recently published results over both Amazonian (Baker et al., 2004) and African (Lewis et al., 2009) forests, suggesting that the observed trends may be local and/or contingent on various environmental and human drivers. In general, research plots can provide samples of how local effects may impact the changes of forest biomass from disturbance and recovery and other ecological processes. However, quantifying regional- to continental-scale processes and trends requires a more balanced and statistical sampling of forests along a wide range of landscape and environmental gradients.

In BCI, the loss of biomass in the old growth forest has been attributed to climate disturbance and drought from 1998 El Niño and subsequent changes in forest composition (Chave et al., 2008; Feeley et al., 2011; Pan et al., 2011). Other factors such as the increasing distribution of lianas in this forest may also help explain partial loss of forest biomass (Wright et al., 2004; Schnitzer et al., 2012). In general, as lianas become more dominant, they tend to impose a higher load on trees, resulting in increasing the risk of the tree falling (Phillips et al., 2002).

Droughts have been considered as the main culprit for the biomass loss in tropical forests, even though other processes may explain this phenomenon (Nepstad et al., 2007; Phillips et al., 2009; Lewis et al., 2011; Saatchi et al., 2013). In most studies, it was hypothesized that the biomass from a severe drought event can be followed with recovery and biomass gain immediately or after few years (Phillips et al., 2009). Here we show that the loss in biomass is gradual, a result consistent with recent remote sensing observations in Amazonia (Saatchi et al., 2013).

A detailed analysis of the field inventory data suggests that the largest decline in biomass has been in DBH classes larger than 40 cm with the most significant loss ( $46.2 \text{ Mg ha}^{-1}$ ) in trees greater than 70 cm in diameter that include primarily the canopy or emergent trees (Fig. 9). Drought has been associated with mortality of large trees in tropical forests in the literature (Nakagawa et al., 2000; Nepstad et al., 2007; Phillips et al., 2009), but this observation is also consistent with the increasing liana load in large trees. Figure 10 shows the dynamics of trees greater than 70 cm in diameter between 2000 and 2010 in the 50 ha plot. Although the number of trees in this DBH class is similar on both dates (526 trees in 2000, 524 trees in 2010), a large turnover was observed during that period. Ground inventory data show that 109 trees died after 2000 while 107 trees entered the 70 cm DBH class by 2010, hence the large biomass loss for this DBH class shown in Fig. 9. Note that the mortality of a big tree has a significant impact on biomass loss, while the growth of a tree to a 70 cm DBH class from a lower DBH class over the same period has a relatively smaller impact on the biomass change. This result is also reflected in the quantification of biomass change versus the biomass levels, showing that subplots with larger biomass values had significantly higher loss (Fig. 3).

### 5.1 Use of lidar height metrics

Our results do not show significant relationships between change in RH and differences in forest biomass derived from the analysis of field surveys. Hence, we were unable to map the changes of forest biomass by directly analyzing the lidar heights at 1 ha scale using two different sensors. Using the same sensor for both dates can potentially provide a more reliable height difference to calculate AGB change directly from lidar, particularly over secondary forests (Dubayah et al., 2010). The indirect estimate of biomass change from lidar

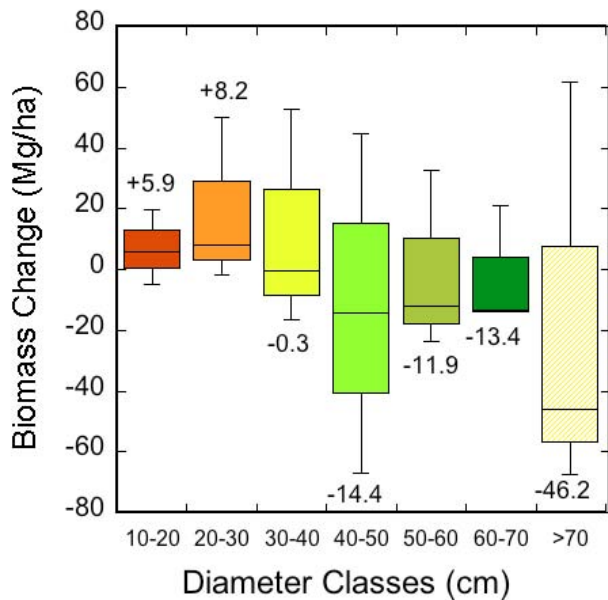


**Fig. 9.** DBH classes and AGB change (20 m spatial scale). AGB is increasing in small DBH classes while trees having DBH higher than 40 m are losing biomass.

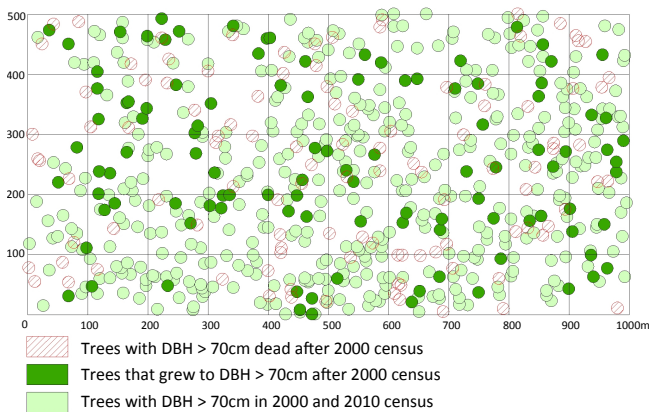


**Fig. 10.** Dynamics of big trees (DBH > 70 cm) in the 50 ha plot between 2000 and 2010. A total of 109 big trees died between 2000 and 2010, while 107 trees entered that DBH class during that time.

data could potentially provide similar results as in inventory data when using larger plots (> 10 ha). By segmenting the lidar-derived biomass changes in the 50 ha plot into different biomass classes, the predicted changes point to regions of old growth with higher biomass values, suggesting plots with potentially larger trees and higher biomass had significantly larger loss in biomass (Fig. 11).

We tested the performance of several AGB estimation models and concluded that, for our datasets, using several height metrics or using a single height metric such as mean canopy height had similar performances in terms of model fitting and RMSE. However, both models present some advantages and drawbacks. Although different height metrics

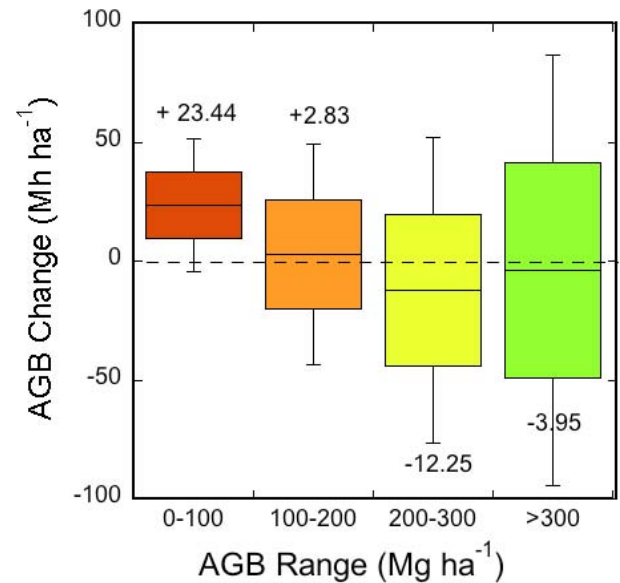


**Fig. 11.** Lidar-derived AGB range and AGB change (20 m spatial scale). AGB in subplots with low biomass is increasing, while subplots with high biomass are losing biomass and contribute to the overall loss of biomass in BCI.

are correlated, each may provide a slightly different slice of vertical structure of the forest canopy and together they improve detection of variation in basal area, tree density, and the structural representation of wood-specific gravity (trees in different diameter classes or successional states). The dynamics of these combined height metrics, if accurately quantified, may provide a more accurate picture of how forests are growing than can be obtained with a single metric. Our comparative results of AGB change over BCI using one approach based on five relative height metrics and another approach based on MCH only are consistent with this hypothesis, although it should be noted that the latter model is more parsimonious. The fact that we detect higher AGB change in the secondary forest when using five metrics than just MCH might be explained by the important contribution of the intermediate height metrics in secondary forests, especially RH25 and RH50. On the other hand, RH100 and MCH are good indicators of AGB loss in the case of a tree fall, but they will be less affected by regrowth than RH25 and RH50. One caveat about using the various height metrics in LVIS data is the fact that they are energy-based and cannot be compared readily with similar metrics from small footprint lidar data. However, using only maximum canopy height to create percentile metrics based on height distribution at pixel level can potentially provide comparable metrics from two different small footprint sensors for change detection.

## 5.2 Spatial scale of forest dynamics

The linear relationship between lidar metrics and biomass estimates was found to be stronger as the pixel scale became coarser. High coefficients of correlation ( $R^2$  ranging between 0.66 and 0.71) and low RMSE ( $\text{RMSE}_{\text{mean}} = 27.6 \text{ Mg ha}^{-1}$ ) indicate that the 1 ha scale is the best spatial scale to use in this type of analysis, as it gives more accurate results and minimizes the errors related to both field data and remote sensing data. At a 0.04 ha scale, we found a poor correlation ( $r_{\text{LVIS}}^2 = 0.19$  and  $r_{\text{DRL}}^2 = 0.28$ ) between ground-estimated AGB and lidar-estimated AGB because the relationship is affected by high AGB variation due to factors such as tree falls, compositional variation and gap regeneration, not necessarily detected to the same accuracy in the field data and the lidar data. Although one could argue that a 0.04 ha spatial scale would be useful in studies related to gap analysis, such a small scale is not necessary for our study and AGB change analyses. It is possible that new generation lidar sensors with increased cloud point density may help reduce the study grain, but probably not below the 0.25 ha scale.

Tree geolocation errors on the ground and tree crown position relative to trunk position are other sources of error. These issues are magnified as the subplot size decreases (Fig. S7). The aggregate effects of these small-scale changes in larger plots or at the stand level define the forest carbon dynamics at annual or multi-year temporal scales.

An encouraging result of this study is that the levels of accuracy for AGB estimates from DRL and LVIS are similar, in spite of differences in sensor design, spatial resolution and footprint size. It opens possibilities in terms of biomass change detection using lidar data for future studies. Although it is always preferable to perform a change analysis using matching datasets at two different dates, our study shows that it is possible to perform this type of analysis using different sensors without affecting the quality of the results.

However, the noise at 1 ha scale is too large to assess biomass change accurately and quantitatively at the plot level. Small changes in biomass are difficult to model at this scale. As a result, average changes at the plot level may be difficult to establish accurately, unless the changes are large. Still, we were able to estimate the change qualitatively and predict the sign of the biomass change (biomass gain or biomass loss) in between 60 % and 64 % of the 1 ha subplots.

In recent studies, Mascaro et al (2011a, b) analyzed error predictions in terms of AGB and carbon stocks over BCI using airborne lidar and ground inventory data. They found that spatial errors scale with the inverse of the square root of pixel area as spatial resolution changes, a result consistent with sampling theory. They then analyzed the importance of plot-edge discrimination errors in AGB estimations and developed a crown correction for localized stems at the edges of the plots to improve the AGB estimation error. They found an RMSE of  $17 \text{ Mg C ha}^{-1}$  for 0.1 and 0.36 ha plots (Mascaro et al., 2011a) covering young and old secondary forests,

and  $11.1 \text{ Mg C ha}^{-1}$  at 1 ha plots (Mascaro et al., 2011b). Their estimates correspond to an RMSE of  $34 \text{ Mg ha}^{-1}$  in terms of AGB at 1 ha. This result is similar to ours, since we found a mean RMSE of  $27.6 \text{ Mg ha}^{-1}$  at the same scale by only focusing on the old growth plots. They further suggest that this RMSE could be reduced by accounting for canopy shape, which is essentially accounting for edge effects in small subplots. Although this is a sensible approach, we refrained from implementing it because crown shape and size are seldom available in ground datasets, and we feel that the uncorrected RMSE reflects more accurately the inherent ability of the lidar technology to infer tropical forest AGB. Further, at the 1 ha scale, this correction results only in a marginal reduction of the error (Mascaro et al., 2011a, Fig. S6), with corrected RMSE of 10.7 against uncorrected RMSE of  $11.1 \text{ Mg C ha}^{-1}$ .

Another difference of our study with that of Mascaro et al. (2011a) is that they used a calibration model between a single lidar metric (MCH) and AGB, including early successional forest plots far away from BCI. Although this would be helpful to map AGB of the whole Panama Canal Zone, it results in artificially inflating the  $R^2$  of the MCH model when just mapping the region at 1 ha. Here we also used five lidar-derived height metrics to estimate AGB directly from data of the 50 ha plot only, providing error estimates for mapping the old growth forest biomass. Our approach also helps counter-balance the effects caused by the limited AGB range in the plot. Because the permanent plot is located in an old growth forest, there was no low biomass subplot. Our approach using a calibration model between MCH and AGB shows that it is possible to estimate AGB using a single-metric model, but the results at the landscape scale suggest that such a model does not detect as much AGB change as the five-metrics model, especially in secondary forests.

## 5.3 Variation of forest dynamics across the island

Landscape-level AGB changes at 1 ha resolution of the old growth and younger forest match changes expected from forest succession theory (Shugart, 1984). Mean AGB change over the whole island was found to be  $+1.5 \text{ Mg ha}^{-1}$  between 2000 and 2010, with most of the old growth forest being neutral or losing AGB (average change =  $-6.8 \text{ Mg ha}^{-1}$ ) while secondary forests gained biomass (average change =  $18.4 \text{ Mg ha}^{-1}$ ) (results from the model using five metrics). Previous ground-based studies over the BCI plot already reported this trend for the 2000–2005 interval (Chave et al., 2008). The fact that 100 yr old secondary forests still are aggrading carbon also is an important finding of this study.

Mascaro et al. (2011a) recently published an AGB map of BCI based on a similar approach. They found that AGB was lower in young forests than in mature forests. Here, we provide the first map of AGB changes and we show that young forests are increasing in AGB.

Dubayah et al. (2010) performed the first AGB change study in a tropical forest. Their study was conducted at La Selva Biological Station, Costa Rica. Their study presents some major differences with our study in terms of methodology. Dubayah et al. (2010) compared two LVIS datasets for the change analysis, while we are comparing one small footprint DRL and one medium footprint LVIS dataset. In their study, Dubayah et al. (2010) performed a footprint-to-footprint comparison of the data and of height metrics. Their approach made it simpler to conduct an AGB change analysis by directly using change in lidar-derived height between two dates, and change in ground-estimated AGB between two dates. Our approach was less direct, but we avoided the issue of DEM location in LVIS. In doing so, we set the stage for forthcoming lidar studies based on a range of operating instruments, including satellite-borne ones. In spite of these differences, the results of Dubayah et al. (2010) and ours are comparable in terms of AGB change trends. Indeed, Dubayah et al. (2010) showed that old growth forest was mostly neutral (average AGB change between 1998 and 2005 of  $+1.9 \text{ Mg ha}^{-1}$ ), while secondary forests were gaining biomass (average change between 1998 and 2005 of  $+25.2 \text{ Mg ha}^{-1}$ ).

#### 5.4 Sources of uncertainty

Estimation of uncertainty in our study and the propagation of errors from field data collection to remote sensing analysis is a difficult task due to the lack of information from various sources of data. However, here we outline and quantify several sources of uncertainty that are contributing in detecting changes of forest biomass from ground and lidar data. We assumed that lidar height metrics may be used to detect biomass changes in old-growth and undisturbed tropical forests. An underlying hypothesis is that changes in biomass in the forest are related to changes in forest height or vertical structure. Unfortunately, this hypothesis is difficult to test based on literature data. Long-term studies in BCI and other sites have revealed that changes in forest structure and dynamics have complex trajectories and are often driven by many factors including random population fluctuations, climate disturbance, large-scale successional or gap phase processes, and increasing resource availability or carbon fertilization (Baker et al., 2004; Chave et al., 2008; Clark et al., 2003, 2010; Feeley et al., 2011; Lewis et al., 2004, 2009). The collective impact of these effects is not necessarily a uniform change in forest structure. In general, over the past 25 yr, the BCI plot has seen a high turnover, with almost 50 % of the initial individuals dying and being replaced.

Some limitations related to both field data and lidar data need to be discussed to understand better our results and errors we have reported throughout the paper. We divide these errors into three categories.

#### 5.4.1 Uncertainty of ground-estimated AGB

The errors associated with the field data are difficult to quantify in this analysis. However, the main errors associated with the estimation of AGB at subplot scales of 1 ha are from three major categories:

1. There are measurement errors related to anomalous DBH values in the inventory plots. These errors are readily identified when multiple census data are available, as in CTFS plots. In this study we assumed that trees that increased in diameter by more than  $45 \text{ mm/yr}$  or shrank more than  $-5 \text{ mm yr}^{-1}$  were inaccurately measured in the field (Chave et al., 2008). For these individuals, the diameter measurement is corrected by assuming a mean growth rate for the individuals in the same diametric class (in millimeters). We assume this approach can introduce a small relative error in AGB estimation at large plots ( $> 1 \text{ ha}$ ). Errors associated with DBH measurements were quantified in Chave et al. (2003, 2004). Using more than two census intervals, as in the case of BCI CTFS plots, will reduce the errors in estimating AGB and AGB change.
2. There are errors associated with the allometry of converting the measurements (DBH, height and wood-specific gravity) to estimate AGB. Chave et al. (2004) have outlined an error propagation approach to quantify the allometric errors at the plot scale and provided relative errors associated with the allometric equation used in this paper elsewhere (Chave et al., 2005). In this study, we are using the moist forest allometry using DBH, height, and wood-specific gravity of tree species (Chave et al., 2005). As we do not measure height of all trees within the 50 ha plot, we have used a model to estimate height from a DBH–height model (see supplementary material). Based on these results, the allometry error at 1 ha plot can be as large as 20 % of the mean.
3. There are geometrical errors associated with the errors in tree location and the plot grid defined by the GIS shape file overlaying the BCI grid. Assuming approximately 1–2 m errors in tree location relative to the plot boundary allows estimation errors at the plot scale.

We have simulated the error associated for all three sources of errors by bootstrap samples drawn 100 times from 1 ha size plots. The relative error associated with geolocation averages to about 1.9 % of the mean AGB and is much smaller than the allometric errors.

Overall, the error associated with allometry is larger than measurement and geolocation errors. Using a simple equation for propagating the errors for ground estimation of biomass in the form of

$$\varepsilon_{\text{AGB}} = \left( \varepsilon_{\text{measurement}}^2 + \varepsilon_{\text{allometry}}^2 + \varepsilon_{\text{geolocation}}^2 \right)^{\frac{1}{2}}, \quad (3)$$

we expect to have errors on the order of 20 % in ground-estimated AGB at 1 ha scale.

#### 5.4.2 Uncertainty in lidar measurements

Several factors introduce errors in lidar estimation of AGB. First, the time difference between the field inventory and the acquisition of lidar data is a source of error that is hard to quantify in our analysis. Events such as tree falls happened between 1998 (LVIS data acquisition) and 2000 and between 2009 (DRL data acquisition) and 2010, causing errors in model calibration, particularly at smaller scales, where the entire subplot can be affected by one tree fall. Other factors such as geolocation error ( $\sim 1$  m) depending on the sensor and sampling errors due to the type of the sensor can become important error sources. In our study, LVIS data had an average of more than 60 shots of 20 m footprint within 1 ha. These samples were not uniform in each plot, and there were gaps within the plot that were not covered in any of LVIS shots. The low number and non-uniform sampling coverage suggest that, on average, about 80 % of the plots were covered by LVIS shots. The sampling error can be as large as 20 % in capturing forest structure in 1 ha plots. This error will impact the direct change detection approach presented in the paper when relating the plot level height difference to AGB difference in the field. However, when using the ground-estimated AGB to calibrate the lidar data, such sampling errors will be integrated into the lidar height biomass estimation model. Note that the error associated with the footprint level sampling at the plot scale is negligible when using DRL data. However, in our analysis the relationship between height metrics and AGB was almost the same for both sensors, suggesting that the errors associated with lidar height biomass allometry models probably dominate the sampling errors present in LVIS data.

#### 5.4.3 Uncertainty in lidar AGB estimation

Our study is also limited by the fact that our calibration excluded young secondary forest plots. Our allometric equation and our regression models were created using the 50 ha plot data, located in a mostly old secondary and old growth forest. The model was then applied to the entire island, composed of both old growth and secondary forests, especially on the eastern part of the island. As a result, our model should predict old growth forest areas better than secondary forest areas. To improve the model, it would be important to establish forest plots in the secondary forest on BCI. The magnitude of lidar prediction error of AGB is approximately 12 % for both LVIS and DRL. This error includes errors associated with sampling and other measurement errors. Using five height metrics, we found negligible bias in estimating AGB relative to the ground-estimated AGB. The random error allows aggregating the uncertainty over larger areas. The average error can reduce to about 5 % at 10 ha and less than 3 % at 25 ha,

suggesting a more reasonable change detection approach by two lidar sensors at  $> 10$  ha if changes of the AGB at this scale exceed 5 % of the mean AGB. We assume the error from lidar estimation of biomass change will decrease when using the same sensor characteristics and observations contemporaneous with the field data.

In the absence of a more reliable uncertainty analysis of all sources of errors in detecting changes of AGB over the landscape, our results can only direct us to general conclusions about the potential of lidar data for detecting changes of AGB: (1) ground-estimated AGB change at 1 ha can have large errors due to measurement and allometric errors that can potentially be reduced using larger plot sizes such as 10–25 ha. However, detailed landscape analysis of AGB change is required to quantify the scale where changes of biomass can be detected from field inventory data. (2) lidar data calibrated with ground-estimated AGB can detect changes of AGB at scales of 10–25 ha depending on the errors assuming the uncertainty in ground-estimated AGB is small. (3) Our results suggest that the ground-estimated AGB error dominates the overall uncertainty of change detection from lidar data, but potential landscape-scale analysis can be performed given the current state of AGB allometry and lidar accuracy at scales of about 10–25 ha. However, we recommend dedicated experiments to improve the understanding and quantification of uncertainty for both ground and remote sensing detection of changes of AGB.

## 6 Conclusions

This study shows that lidar can be used to analyze tropical forest dynamics on a decadal scale. Unlike other remote sensing technologies, lidar is able to provide information on vertical forest structure, which makes it a unique tool to study and understand AGB and its dynamics through time at the landscape scale. Although AGB changes are hard to quantify at the plot level using lidar data only, scaling up these changes at a landscape scale is a fundamental objective to understand the dynamics of forest succession. We demonstrated that there is no advantage in using spatial scales that belong to the same range as tree crown sizes when estimating AGB change, especially at a landscape scale. Spatial scales below 1 ha are dominated by uncertainty in ground estimation of AGB, plot-edge effects and by the differences in sensor characteristics. Spatial scales, typically on the order of 1 ha, give more accurate results and should be preferred to finer scales in future studies.

**Supplementary material related to this article is available online at: <http://www.biogeosciences.net/10/5421/2013/bg-10-5421-2013-supplement.pdf>.**

**Acknowledgements.** The research was carried out at the Jet Propulsion Laboratory, California Institute of Technology, under a contract with the National Aeronautics and Space Administration. We would like to thank the reviewers for their constructive comments and recommendations. We are grateful for insightful comments from Helene Muller-Landau. We thank Richard Condit for providing the field data (2010). The BCI forest dynamics research project was made possible by National Science Foundation grants to Stephen P. Hubbell, support from the Center for Tropical Forest Science, the Smithsonian Tropical Research Institute, the John D. and Catherine T. MacArthur Foundation, the Mellon Foundation, the Small World Institute Fund, and numerous private individuals, and through the hard work of over 100 people from 10 countries over the past two decades. The DRL dataset was obtained with funding from NSF grant 0939907, and with additional support from the Smithsonian Tropical Research Institute, University of Illinois, University of California Los Angeles, and Clemson University to S.J. DeWalt. This work has benefited from French “Investissement d’avenir” grants (CEBA: ANR-10-LABX-0025; TULIP: ANR-10-LABX-0041) and from TOSCA funds (CNES, France).

Edited by: M. Williams

## References

- Asner, G. P., Powell, G. V. N., Mascaro, J., Knapp, D. E., Clark, J. K., Jacobson, J., Kennedy-Bowdoin, T., Balaji, A., Paez-Acosta, G., Victoria, E., Secada, L., Valqui, M., and Hughes, R. F.: High-resolution forest carbon stocks and emissions in the Amazon, *P. Natl. Acad. Sci. USA*, 107, 16738–16742, 2010.
- Asner, G. P., Hughes, R. F., Mascaro, J., Uowolo, A., Knapp, D. E., Jacobson, J., Kennedy-Bowdoin, T., Clark, J. K., and Balaji, A.: High-resolution carbon mapping on the million-hectare Island of Hawaii, *Front. Ecol. Environ.*, 8, 434–439, doi:10.1890/100179, 2011.
- Baker, T. R., Phillips, O. L., Malhi, Y., Almeida, S., Arroyo, L., Di Fiore, A., Erwin, T., Higuchi, N., Killeen, T. J., Laurance, S. G., Laurance, W. F., Lewis, S. L., Monteagudo, A., Neill, D. A., Vargas, P. N., Pitman, N. C. A., Silva, J. N. M., and Martínez, R. V.: Increasing biomass in Amazonian forest plots, *Philos. T. Roy. Soc. Lond. B*, 359, 353–365, 2004.
- Bohlman, S. and O’Brien, S.: Allometry, adult stature and regeneration requirement of 65 tree species on Barro Colorado Island, Panama, *J. Trop. Ecol.*, 22, 123–136, 2006.
- Chambers, J. Q., dos Santos, J., Ribeiro, R. J., and Higuchi, N.: Tree damage, allometric relationships, and above-ground net primary production in central Amazon forest, *Forest Ecol. Manag.*, 152, 73–84, 2001.
- Chao, Y. C. E., Zhao, Y., Kupper, L. L., and Nylander-French, L. A.: Quantifying the relative importance of predictors in multiple linear regression analyses for public health studies, *J. Occup. Environ. Hyg.*, 5, 519–529, 2008.
- Chave, J., Condit, R., Lao, S., Caspersen, J. P., Foster, R. B., and Hubbell, S. P.: Spatial and temporal variation of biomass in a tropical forest: results from a large census plot in Panama, *J. Ecol.*, 91, 240–252, 2003.
- Chave, J., Condit, R., Aguilar, S., Hernandez, A., Lao, S., and Perez, R.: Error propagation and scaling for tropical forest biomass estimates, *Philos. T. Roy. Soc. Lond. B*, 359, 409–420, 2004.
- Chave, J., Andalo, C., Brown, S., Cairns, M., Chambers, J., Eamus, D., Folster, H., Fromard, F., Higuchi, N., Kira, T., Lescure, J. P., Nelson, B., Ogawa, H., Puig, H., Riera, B., and Yamakura, T.: Tree allometry and improved estimation of carbon stocks and balance in tropical forests, *Oecologia*, 145, 87–99, 2005.
- Chave, J., Condit, R., Muller-Landau, H. C., Thomas, S. C., Ashton, P. S., Bunyavechewin, S., Co, L. L., Dattaraja, H. S., Davies, S. J., Esufali, S., Ewango, C. E. N., Feeley, K. J., Foster, R. B., Gunatilleke, N., Gunatilleke, S., Hall, P., Hart, T. B., Hernandez, C., Hubbell, S. P., Itoh, A., Kiratiprayoon, S., LaFrankie, J. V., de Lao, S. L., Makana, J. R., Noor, M. N. S., Kasim, A. R., Samper, C., Sukumar, R., Suresh, H. S., Tan, S., Thompson, J., Tongco, M. D. C., Valencia, R., Vallejo, M., Villa, G., Yamakura, T., Zimmerman, J. K., and Losos, E. C.: Assessing evidence for a pervasive alteration in tropical tree communities, *Plos Biol.*, 6, 455–462, 2008.
- Chazdon, R. L.: Tropical forest recovery: legacies of human impact and natural disturbances, *Perspect. Plant Ecol.*, 6, 51–71, 2003.
- Clark, D. B. and Clark, D. A.: Landscape-scale variation in forest structure and biomass in a tropical rain forest, *Forest Ecol. Manag.*, 137, 185–198, 2000.
- Clark, D. A., Piper, S. C., Keeling, C. D., and Clark, D. B.: Tropical rain forest tree growth and atmospheric carbon dynamics linked to interannual temperature variation during 1984–2000, *P. Natl. Acad. Sci. USA*, 100, 5852–5857, 2003.
- Clark, D. B., Clark, D. A., and Oberbauer, S. F.: Annual wood production in a tropical rain forest in NE Costa Rica linked to climatic variation but not to increasing CO<sub>2</sub>, *Glob. Change Biol.*, 16, 747–759, 2010.
- Condit, R.: Research in large, long-term tropical forest plots, *Trends Ecol. Evol.*, 10, 18–22, 1995.
- Condit, R.: *Tropical Forest Census Plots*. Springer-Verlag and R. G. Landes Company, Berlin, Germany, and Georgetown, Texas, 1998.
- Condit, R., Watts, K., Bohlman, S. A., Perez, R., Foster, R. B., and Hubbell, S. P.: Quantifying the deciduousness of tropical forest canopies under varying climates, *J. Veg. Sci.*, 11, 649–658, 2000.
- Croat, T. B.: *Flora of Barro Colorado Island*, Stanford University Press, Stanford, CA, 1978.
- Dalling, J. W., Schnitzer, S. A., Baldeck, C., Harms, K. E., John, R., Mangan, S. A., Lobo, E., Yavitt, J. B., and Hubbell, S. P.: Resource-based habitat associations in a neotropical liana community, *J. Ecol.*, 100, 1174–1182, 2012.
- Drake, J. B., Dubayah, R. O., Clark, D. B., Knox, R. G., Blair, J. B., Hofton, M. A., Chazdon, R. L., Weishampel, J. F., and Prince, S.: Estimation of tropical forest structural characteristics using large-footprint lidar, *Remote Sens. Environ.*, 79, 305–319, 2002a.
- Drake, J. B., Dubayah, R. O., Knox, R. G., Clark, D. B., and Blair, J. B.: Sensitivity of large-footprint lidar to canopy structure and biomass in a neotropical rainforest, *Remote Sens. Environ.*, 81, 378–392, 2002b.
- Drake, J. B., Knox, R. G., Dubayah, R. O., Clark, D. B., Condit, R., Blair, J. B., and Hofton, M.: Above-ground biomass estimation in closed canopy Neotropical forests using lidar remote sensing: factors affecting the generality of relationships, *Global Ecol. Biogeogr.*, 12, 147–159, 2003.

- Dubayah, R. O., Sheldon, S. L., Clark, D. B., Hofton, M. A., Blair, J. B., Hurr, G. C., and Chazdon, R. L.: Estimation of tropical forest height and biomass dynamics using lidar remote sensing at La Selva, Costa Rica, *J. Geophys. Res.*, 115, G00E09, doi:10.1029/2009JG000933, 2010.
- Duong, V. H., Lindenbergh, R., Pfeifer, N., and Vosselman, G.: Single and two epoch analysis of ICESat full waveform data over forested areas, *Int. J. Remote Sens.*, 29, 1453–1473, 2008.
- Enders, R. K.: Mammalian life histories from Barro Colorado Island, Panama, *Bull. Mus. Comp. Zool.*, 78, 385–502, 1935.
- Feeley, K. J., Davies, S. J., Perez, P., Hubbell, S., and Foster R.: Directional changes in the species composition of a tropical forest, *Ecology*, 92, 871–882, 2011.
- Foster Jr., R. B.: Structure and history of the vegetation of Barro Colorado Island, in: *The Ecology of a Tropical Forest Seasonal Rhythms and Long-Term Changes*, edited by: Brokaw, N., Smithsonian Institution Press, Washington DC, 67–82, 1982.
- Fricker, G. A., Saatchi, S. S., Meyer, V., Gillespie, T. W., and Sheng, Y.: Application of semi-automated filter to improve waveform Lidar sub-canopy elevation model, *Remote Sens.*, 4, 1494–1518, 2012.
- Higuchi, N., Santos, J. M., Imanaga, M., and Yoshida, S.: Above-ground Biomass Estimate for Amazonian Dense Tropical Moist Forests, *Memoirs of the Faculty of Agriculture, Kagoshima*, 30, 43–54, 1994.
- Hofton, M. A., Rocchio, L. E., Blair, J. B., and Dubayah, R.: Validation of Vegetation Canopy Lidar sub-canopy topography measurements for a dense tropical forest, *J. Geodyn.*, 34, 491–502, 2002.
- Hubbell, S. P. and Foster, R. B.: Diversity of canopy trees in a neotropical forest and implications for conservation, in: *Tropical Rain Forest: Ecology and Management*, edited by: Sutton, S. L., Whitmore, T. C. and Chadwick, A. D., 25–41. Blackwell Scientific, Oxford, 1983.
- Hubbell, S. P., Foster, R. B., O'Brien, S. T., Harms, K. E., Condit, R., Wechsler, B., Wright, S. J., and Loo de Lao, S.: Light gap disturbances, recruitment limitation, and tree diversity in a neotropical forest, *Science* 283: 554–557, 1999.
- Hubbell, S. P., Condit, R., and Foster, R. B.: Barro Colorado Forest Census Plot Data, <https://ctfs.arnarb.harvard.edu/webatlas/datasets/bci>, 2005.
- Kellner, J. R. and Asner, G. P.: Convergent structural responses of tropical forests to diverse disturbance regimes, *Ecol. Lett.*, 12, 887–897, 2009.
- Kenoyer, L. A.: General and successional ecology of the lower tropical rain-forest at Barro Colorado Island, Panama, *Ecology*, 10, 201–222, 1929.
- Lefsky, M. A., Cohen, W. B., Parker, G. G., and Harding, D. J.: Lidar remote sensing for ecosystem studies, *BioScience*, 52, 19–30, 2002.
- Leigh, E. G.: *Tropical Forest Ecology: A View from Barro Colorado Island*, Oxford University Press, New York Oxford, 1999.
- Leigh, E. G. and Wright, S. J.: Barro Colorado Island and tropical biology, in: *Four Neotropical Rainforests*, edited by: Gentry, A. H., Yale University Press, New Haven, USA, 28–47, 1990.
- Leigh, E. G., Loo de Lao, S., Condit, R. G., Hubbell, S. P., Foster, R. B., and Perez, R.: Barro Colorado Island forest dynamics plot, Panama, in: *Tropical Forest Diversity and Dynamism: Findings from a Large-Scale Plot Network*, edited by: Losos, E. C. and Leigh, J., Egbert Giles, University of Chicago Press, Chicago, 451–463, 2004.
- Lewis, S. L., Malhi, Y., and Phillips, O. L.: Fingerprinting the impacts of global change on tropical forests, *Philos. T. Roy. Soc. B*, 359, 437–462, 2004.
- Lewis, S. L., Lopez-Gonzalez, G., Sonke, B., Affum-Baffoe, K., Baker, T. R., Ojo, L. O., Phillips, O. L., Reitsma, J. M., White, L., Comiskey, J. A., Djukouo, M. N., Ewango, C. E. N., Feldpausch, T. R., Hamilton, A. C., Gloor, M., Hart, T., Hladik, A., Lloyd, J., Lovett, J. C., Makana, J.-R., Malhi, Y., Mbago, F. M., Ndagalasi, H. J., Peacock, J., Peh, K. S. H., Sheil, D., Sunderland, T., Swaine, M. D., Taplin, J., Taylor, D., Thomas, S. C., Votere, R., and Woll, H.: Increasing carbon storage in intact African tropical forests, *Nature*, 457, 1003–1006, 2009.
- Lewis, S. L., Brando, P. M., Phillips, O. L., van der Heijden, G. M., and Nepstad, D.: The 2010 amazon drought. *Science*, 331, 554–554, 2011.
- Mascaró, J., Asner, G. P., Muller-Landau, H. C., van Breugel, M., Hall, J., and Dahlin, K.: Controls over aboveground forest carbon density on Barro Colorado Island, Panama, *Biogeosciences*, 8, 1615–1629, doi:10.5194/bg-8-1615-2011, 2011a.
- Mascaró, J., Detto, M., Asner, G. P., and Muller-Landau, H. C.: Evaluating uncertainty in mapping forest carbon with airborne Lidar, *Remote Sens. Environ.*, 115, 3770–3774, 2011b.
- McCullough, D.: *The Path Between the Seas*, Simon and Schuster, New York, NY, USA, 1977.
- Nakagawa, M., Tanaka, K., Nakashizuka, T., Ohkubo, T., Kato, T., Maeda, T., Sato, K., Miguchi H., Nagamasu H., Ogino K., Teo S., Hamid A. A., and Seng L. H.: Impact of severe drought associated with the 1997–1998 El Niño in a tropical forest in Sarawak, *J. Trop. Ecol.*, 16, 355–367, 2000.
- Nepstad, D. C., Tohver, I. M., Ray, D., Moutinho P., and Cardinot, G.: Mortality of large trees and lianas following experimental drought in an Amazon forest, *Ecology*, 88, 2259–2269, 2007.
- Ni-Meister, W., Jupp, D. L. B., and Dubayah, R.: Modeling Lidar waveforms in heterogeneous and discrete canopies, *IEEE T. Geosci. Remote*, 39, 1943–1958, 2001.
- Pan, Y., Birdsey, R. A., Fang, J., Houghton, R., Kauppi, P. E., Kurz, W. A., Phillips, O. L., Shvidenko A., Lewis, S. L., Canadell, J. G., Ciais, P., Jackson R. B., Pacala S. W., McGuire A. D., Piao, S., Rautiainen, A., Sitch, S., and Hayes, D.: A Large and Persistent Carbon Sink in the World's Forests, *Science*, 333, 988–993, doi:10.1126/science.1201609, 2011.
- Phillips, O. L., Malhi, Y., Higuchi, N., Laurance, W. F., Núñez, P. V., Vásquez, R. M., Laurance S. G., Ferreira L. V., Stern M., Brown S., and Grace J.: Changes in the carbon balance of tropical forests: evidence from long-term plots, *Science*, 282, 439–442, 1998.
- Phillips, O. L., Martínez, R. V., Arroyo, L., Baker, T. R., Killeen, T., Lewis, S. L., Malhi Y., Mendoza, A. M., Neill D., Núñez P. V., Alexiades M., Cerón C., Di Fiore A., Erwin T., Jardim A., Palacios W., Saldias M., and Vinceti, B.: Increasing dominance of large lianas in Amazonian forests, *Nature*, 418, 770–774, 2002.
- Phillips, O. L., Aragão, L. E., Lewis, S. L., Fisher, J. B., Lloyd, J., López-González, G., Malhi, Y., Monteagudo A., Peacock J., Quesada C.A., van der Heijden G., Almeida S., Amaral I., Arroyo L., Aymard G., Baker T.R., Bánki O., Blanc L., Bonal D., Brando P., Chave J., Alves de Oliveira A. C., Cardozo N. D., Czimeczik C. I., Feldpausch T. R., Freitas M. A., Gloor E., Higuchi

- N., Jiménez E., Lloyd G., Meir P., Mendoza C., Morel A., Neill D. A., Nepstad D., Patiño S., Peñuela M. C., Prieto A., Ramírez F., Schwarz M., Silva J., Silveira M., Thomas A. S., ter Steege H., Stropp J., Vásquez R., Zelazowski P., Dávila E. A., Andelman S., Andrade A., Chao K. J., Erwin T., Di Fiore A., Honorio E., Keeling H., Killeen T. J., Laurance W. F., Cruz A. P., Pitman N. C. A., Vargas P. N., Ramírez-Angulo H., Rudas A., Salamáo R., Silva N., Terborgh J., and Torres-Lezama A.: Drought sensitivity of the Amazon rainforest, *Science*, 323, 1344–1347, 2009.
- Saatchi, S. S., Harris, N. L., Brown, S., Lefsky, M., Mitchard, E. T. A., Salas, W., Zutta, B. R., Buermann, W., Lewis, S. L., Hagen, S., Petrova, S., White, L., Silman, M., and Morel, A.: Benchmark map of forest carbon stocks in tropical regions across three continents, *P. Natl. Acad. Sci. USA*, 108, 9899–9904, 2011.
- Saatchi S. S., Asefi-Najafabady S., Malhi Y., Aragao L. E. O. C., Anderson L.O., Myneni R. B., and Nemani R.: Persistent effects of a severe drought on Amazonian forest canopy, *P. Natl Acad. Sci. USA*, 110, 565–570, doi:10.1073/pnas.1204651110, 2013.
- Schnitzer, S. A., Mangan, S. A., Dalling, J. W., Baldeck, C. A., Hubbell, S. P., Ledo, A., Muller-Landau, H., Tobin, M.F., Aguilar, S., Brassfield, D., Hernandez, A., Lao, S., Perez, R., Valdez, O., and Rutishauser Yorke, S.: Liana abundance, diversity and distribution on Barro Colorado Island, Panama, *Plos One*, 7, e52114, doi:10.1371/journal.pone.0052114, 2012.
- Shugart, H. H.: *A Theory of Forest Dynamics*, Springer, New York, NY, 1984.
- Vincent G., Sabatier D., Blanc L., Chave J., Weissenbacher E., Pélissier R., Fonty E., Molino J.-F., and Coutron P.: Accuracy of small footprint airborne LiDAR in its predictions of tropical moist forest stand structure, *Remote Sens. Environ.*, 125, 23–33, 2012.
- Wright, S. J., Calderón, O., Hernández, A., and Paton, S.: Are lianas increasing in importance in tropical forests? A 17-year record from Panama, *Ecology*, 85, 484–489, 2004.